

Syntheses, Structure, and a Mössbauer and Magnetic Study of $\text{Ba}_4\text{Fe}_2\text{I}_5\text{S}_4$

Danielle L. Gray,[†] Gary J. Long,^{*#} Fernande Grandjean,[‡] Raphaël P. Hermann,^{‡§} and James A. Ibers^{*†}

Department of Chemistry, Northwestern University, Evanston, Illinois 60208-3113, Department of Chemistry, University of Missouri-Rolla, Rolla, Missouri 65409-0010, and Department of Physics, University of Liège, B-4000 Sart-Tilman, Belgium

Received June 1, 2007

The compound $\text{Ba}_4\text{Fe}_2\text{I}_5\text{S}_4$ has been prepared at 1223–1123 K by the “U-assisted” reaction of FeS, BaS, S, and U with BaI_2 as a flux. A more rational synthesis was also found; however, the presence of U appears to be essential for the formation of single crystals suitable for X-ray diffraction studies. $\text{Ba}_4\text{Fe}_2\text{I}_5\text{S}_4$ crystallizes in a new structure type with two formula units in space group $I4/m$ of the tetragonal system. The structure consists of a Ba–I network penetrated by ${}^{\infty}[\text{Fe}_2\text{S}_4]$ chains. Each Fe atom, which is located on a site with $\bar{4}$ symmetry, is tetrahedrally coordinated to four S atoms. The FeS_4 tetrahedra edge-share to form linear ${}^{\infty}[\text{Fe}_2\text{S}_4]$ chains in the [001] direction. The Fe–Fe interatomic distance in these chains is 2.5630(4) Å, only about 3% longer than the shortest Fe–Fe distance in α -Fe metal. Charge balance dictates that the average formal oxidation state of Fe in these chains is +2.5. The Mössbauer spectra obtained at 85 and 270 K comprise a single quadrupole doublet that has hyperfine parameters consistent with an average Fe oxidation state of +2.5. The Mössbauer spectrum obtained at 4.2 K consists of a single magnetic sextet with a small hyperfine field of –15.5 T. This spectrum is also consistent with rapid electron delocalization and an average Fe oxidation state of +2.5. The molar magnetic susceptibility of $\text{Ba}_4\text{Fe}_2\text{I}_5\text{S}_4$, obtained between 3.4 and 300 K, qualitatively indicates the presence of weak pseudo-one-dimensional ferromagnetic exchange within a linear chain above 100 K and weak three-dimensional ordering between the chains at lower temperatures.

Introduction

The Ba/Fe/S system shows a diverse structural chemistry. Structures in the system range from $\text{Ba}_7\text{Fe}_6\text{S}_{14}$ (monoclinic, $C2/c$)¹ to β - BaFe_2S_4 (tetragonal, $I4/m$).² Stoichiometries within the system are just as diverse. These include BaFe_2S_3 ,³ Ba_2FeS_3 ,³ Ba_3FeS_5 ,⁴ $\text{Ba}_5\text{Fe}_4\text{S}_{11}$,⁵ $\text{Ba}_5\text{Fe}_9\text{S}_{18}$,⁶ $\text{Ba}_6\text{Fe}_8\text{S}_{15}$,³ α -

and β - $\text{Ba}_9\text{Fe}_4\text{S}_{15}$,⁷ $\text{Ba}_9\text{Fe}_{16}\text{S}_{32}$,⁸ and $\text{Ba}_{15}\text{Fe}_7\text{S}_{25}$.⁴ These structures are built from FeS_4 tetrahedra that share corners or edges to form trinuclear units, tetranuclear units, chains, or sheets. The structural diversity stems not only from the many ways that the FeS_4 tetrahedra interconnect but also from the variable coordination number of Ba, which in an S environment can range from 6 to 12. Iron oxidation states in these compounds can be difficult to assign. In compounds such as Ba_2FeS_3 , where there are no S–S bonds, the iron oxidation state is easily assigned as +2, an assignment that is confirmed by Mössbauer spectroscopy.⁹ However, in $\text{Ba}_6\text{Fe}_8\text{S}_{15}$ the iron oxidation state averages to +2.25 for the crystallographically indistinguishable iron centers.³ The Mössbauer spectrum of $\text{Ba}_6\text{Fe}_8\text{S}_{15}$ shows only a single quadrupole doublet at both 300 and 195 K with an intermediate isomer shift.⁹

* To whom correspondence should be addressed. E-mail: ivers@chem.northwestern.edu (J.A.I.), glong@umr.edu (G.J.L.).

[†] Northwestern University.

[#] University of Missouri-Rolla.

[‡] University of Liège.

[§] Present address: Institut für Festkörperforschung, Forschungszentrum Jülich, D-52425, Jülich, Germany.

(1) Grey, I. E.; Hong, H.; Steinfink, H. *Inorg. Chem.* **1971**, *10*, 340–343.

(2) Swinnea, J. S.; Steinfink, H. *J. Solid State Chem.* **1980**, *32*, 329–334.

(3) Hong, H. Y.; Steinfink, H. *J. Solid State Chem.* **1972**, *5*, 93–104.

(4) Lemley, J. T.; Jenks, J. M.; Hoggins, J. T.; Eliezer, Z.; Steinfink, H. *J. Solid State Chem.* **1976**, *16*, 117–128.

(5) Cohen, S.; Kimizuka, N.; Steinfink, H. *J. Solid State Chem.* **1980**, *35*, 181–186.

(6) Grey, I. E. *Acta Crystallogr., Sect. B: Struct. Crystallogr. Cryst. Chem.* **1975**, *31*, 45–48.

(7) Cohen, S.; Rendon-Diazmiron, L. E.; Steinfink, H. *J. Solid State Chem.* **1978**, *25*, 179–187.

(8) Hoggins, J. T.; Steinfink, H. *Acta Crystallogr., Sect. B: Struct. Crystallogr. Cryst. Chem.* **1977**, *33*, 673–678.

(9) Reiff, W. M.; Grey, I. E.; Fan, A.; Eliezer, Z.; Steinfink, H. *J. Solid State Chem.* **1975**, *13*, 32–40.

The exploratory nature of solid-state chemistry often leads to the syntheses of unexpected compounds. While exploring the U/Fe/S system in the presence of BaS and BaI₂, a new compound, Ba₄Fe₂I₅S₄, was isolated. Because of the diverse nature of the ternary Ba/Fe/S system, we have further characterized this compound. Herein, we present the syntheses and characterization of Ba₄Fe₂I₅S₄.

Experimental Section

Syntheses. The following reagents were used as obtained: BaS (Alfa Aesar, 99.7%), FeS (Strem, 99.9%), S (Mallinckrodt, 99.6%), and BaI₂ (Strem, 97%). Depleted U turnings (Oak Ridge National Laboratory) were cleaned in a concentrated HNO₃ solution to remove the oxide layer on the surface. The turnings were then quickly rinsed in deionized water and dried with acetone for immediate use. Reaction mixtures were loaded into carbon-coated fused-silica tubes under an Ar atmosphere in a glovebox. These tubes were sealed under a 10⁻⁴ Torr atmosphere and then placed in a computer-controlled furnace. The products of the reactions were consistent with the stated compositions, as determined by the examination of selected single crystals with an energy dispersive X-ray (EDX)-equipped Hitachi S-3500 scanning electron microscope.

Single crystals of Ba₄Fe₂I₅S₄ were obtained from the reaction of 0.130 mmol of BaS, 0.125 mmol of FeS, 0.280 mmol of S, 0.100 mmol of BaI₂, and 0.125 mmol of U. The sample was heated in a two-zone furnace with the reactants in the hot zone. The hot zone was heated to 1223 K in 24 h, kept at 1223 K for 72 h, cooled at 8.3 K/h to 773 K, cooled at 6.25 K/h to 473 K, and then the furnace was turned off. The cooler zone was heated to 1123 K in 24 h, kept at 1123 K for 72 h, cooled at 8.3 K/h to 673 K, cooled at 6.25 K/h to 373 K, and then the furnace was turned off. The products were opened into paratone oil to prevent decomposition from air and moisture. By inspection, about 40% of the product comprised black needles of what turned out to be Ba₄Fe₂I₅S₄. EDX analysis of selected crystals showed an average ratio of Ba/Fe/I/S equal to 4:2:5:4. There was no indication of the presence of U. This reaction is reproducible and affords single crystals of Ba₄Fe₂I₅S₄ of good quality.

In an attempted rational synthetic route, the loading was changed to 0.34 mmol of BaS, 0.23 mmol of FeS, 0.79 mmol of BaI₂, and 0.57 mmol of S. Because at high temperatures BaS reacts with fused silica even through several layers of carbon coating, the heating/cooling sequence was allowed to proceed over several steps. The reaction was heated to 773 K in 1 h, kept at 773 K for 12 h, and then rapidly cooled to 298 K. The contents were removed from the tube in an N₂-atmosphere glovebag, ground, and then reloaded into a fresh carbon-coated tube. This tube was heated to 973 K in 12 h, kept at 973 K for 12 h, and then cooled at 112 K/h to 298 K. The contents were ground again and heated in a fresh fused-silica tube to 973 K in 8 h, kept at 973 K for 48 h, and cooled at 85 K/h. This method yielded no single crystals of Ba₄Fe₂I₅S₄; apparently the presence of U is essential for their formation. Nevertheless, the X-ray diffraction powder pattern of the products is consistent with the presence of 40 wt % Ba₄Fe₂I₅S₄, 7 wt % BaS, 49 wt % BaI₂, and 4 wt % S and the absence of FeS. This powder was used for subsequent Mössbauer and magnetic studies.

Crystallography. Single-crystal X-ray diffraction data were collected with the use of graphite-monochromatized Mo K α radiation ($\lambda = 0.71073$ Å) at 153 K on a Bruker Smart-1000 CCD

Table 1. Crystallographic Details for Ba₄Fe₂I₅S₄

fw, g mol ⁻¹	1423.8	μ , cm ⁻¹	178
Z	2	$R(F)^a$	0.035
space group	<i>I4/m</i>	$R_w(F^2)^b$	0.09
<i>a</i> , Å	13.758(1)	λ (Mo K α), Å	0.71073
<i>c</i> , Å	5.1261(7)	<i>T</i> , K	153(2)
ρ_c , g cm ⁻³	4.873		

^a $R(F) = \sum ||F_o| - |F_c|| / \sum |F_o|$ for $F_o^2 > 2\sigma(F_o^2)$. ^b $R_w(F^2) = [\sum w(F_o^2 - F_c^2)^2 / \sum wF_o^4]^{1/2}$, $w^{-1} = \sigma^2(F_o^2) + (0.03F_o^2)^2$ for $F_o^2 \geq 0$; $w^{-1} = \sigma^2(F_o^2)$ for $F_o^2 < 0$.

Table 2. Selected Distances (Å) and Angles (deg) for Ba₄Fe₂I₅S₄

Fe–S \times 4	2.267(2)	Ba–I(2) \times 2	3.6054(6)
Ba–S	3.195(2)	Ba–I(2)	3.6539(8)
Ba–S \times 2	3.298(1)	Ba–I(2) \times 2	3.7276(6)
Ba–I(1)	3.5132(6)	Fe–Fe	2.5630(4)
S–Fe–S	108.64(3)	I(1)–Ba \times 4	3.5132(6)
S–Fe–S	111.16(6)	Ba–I(1)–Ba	180

diffractometer.¹⁰ The crystal-to-detector distance was 5.023 cm. Crystal decay was monitored by re-collecting 50 initial frames at the end of the data collection; none was observed. Data were collected by scans of 0.3° in ω in groups of 606 frames at φ settings of 0°, 90°, 180°, and 270°. The exposure time was 15 s/frame. The collection of intensity data was carried out with the *SMART* program.¹⁰ Cell refinement and data reduction were carried out with the *SAINTE* program,¹⁰ and face-indexed absorption corrections were performed numerically with the *XPREP*¹¹ program. Because the crystals were fine needles, a Leitz microscope with a calibrated traveling micrometer was employed to measure accurately the crystal faces of the data crystal for a face-indexed absorption correction. Then the *SADABS* program¹⁰ was employed to make incident beam and decay corrections.

The structure was solved with the direct methods *SHELXS* program and refined with the full-matrix least-squares *SHELXL* program.¹¹ The *STRUCTURE TIDY* program¹² was used to standardize the positional parameters. Additional experimental details are given in Table 1 and in the Supporting Information. Selected metrical details are presented in Table 2.

Mössbauer Spectroscopy. The Mössbauer spectral absorbers contained boron nitride mixed with 40 mg/cm² of powdered sample for the 85 and 270 K spectra and 31 mg/cm² of powdered sample for the 4.2 K spectra; separate preparations of Ba₄Fe₂I₅S₄ were used in the two absorbers. The spectra were measured on constant-acceleration spectrometers that utilized a room-temperature rhodium matrix ⁵⁷Co source and were calibrated at room temperature with α -Fe foil. The estimated relative errors are ± 0.005 mm/s for the isomer shifts, ± 0.01 mm/s for the quadrupole splittings and line widths, and ca. ± 0.5 T for the hyperfine field. The absolute errors are estimated to be approximately twice as large.

Magnetic Susceptibility. The dc magnetic susceptibility of Ba₄Fe₂I₅S₄ has been measured on a Quantum Design MPMS5 SQUID magnetometer by using 41.5 mg of ground powder that was placed in a gelatin capsule. The measurements were made between 3.4 and 300 K in a 0.7 T applied field after both zero-field cooling and 0.7 T field cooling. The observed susceptibility has been corrected for the known presence of diamagnetic BaI₂, BaS, and S by using diamagnetic corrections of -0.000136 , -0.000070 , and

(10) *SMART*, version 5.054, *Data Collection* and *SAINTE-Plus*, version 6.454, *Data Processing Software for the SMART System*; Bruker Analytical X-Ray Instruments, Inc.: Madison, WI, 2003.

(11) Sheldrick, G. M. *SHELXTL*, version 6.14; Bruker Analytical X-Ray Instruments, Inc.: Madison, WI, 2003.

(12) Gelato, L. M.; Parthé, E. *J. Appl. Crystallogr.* **1987**, *20*, 139–143.

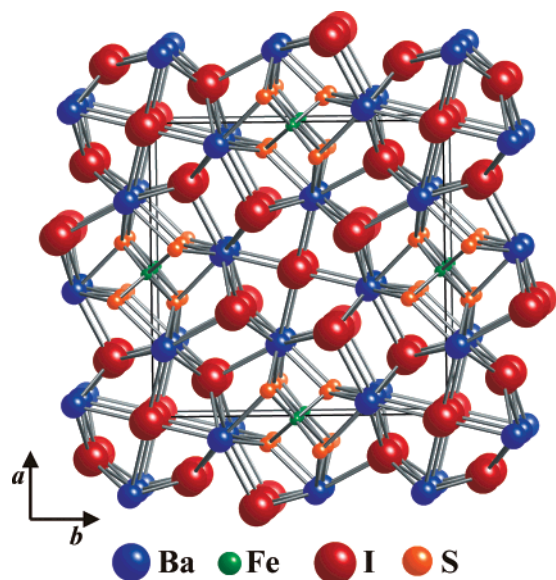


Figure 1. Structure of $\text{Ba}_4\text{Fe}_2\text{I}_5\text{S}_4$ as viewed down [001].

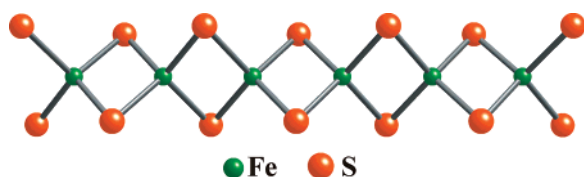


Figure 2. ${}^1_{\infty}[\text{Fe}_2\text{S}_4]$ chain in $\text{Ba}_4\text{Fe}_2\text{I}_5\text{S}_4$ as viewed along [001].

-0.000001 emu/mol, respectively. A correction of -0.000563 emu/mol was then used to obtain the diamagnetic-corrected molar magnetic susceptibility, χ_M' , of $\text{Ba}_4\text{Fe}_2\text{I}_5\text{S}_4$. All of the diamagnetic corrections have been obtained from tables of Pascal's constants.

Results and Discussion

Syntheses. The initial synthesis of $\text{Ba}_4\text{Fe}_2\text{I}_5\text{S}_4$ proceeded from a nonstoichiometric reaction of BaS, BaI_2 , FeS, S, and U in a two-zone furnace with a 100 K gradient between the hot zone at 1223 K and cold zone at 1123 K. This reaction afforded high-quality black needles of $\text{Ba}_4\text{Fe}_2\text{I}_5\text{S}_4$ in approximately 40 wt % yield. Most of these crystals were not separable from the product melt owing in part to their high sensitivity to moisture and atmosphere. A rational synthesis afforded no single crystals but rather a powder sample that was reasonably free of iron impurities. The “U-assisted” growth of single crystals is not without precedent.¹³

Crystal Structure. $\text{Ba}_4\text{Fe}_2\text{I}_5\text{S}_4$ crystallizes in a new structure type (Figure 1) that consists of a Ba–I network penetrated by ${}^1_{\infty}[\text{Fe}_2\text{S}_4]$ chains. Each Fe center, which is located on a site with $\bar{4}$ symmetry, is tetrahedrally coordinated to four S atoms. The FeS_4 tetrahedra edge-share to form linear ${}^1_{\infty}[\text{Fe}_2\text{S}_4]$ chains in the [001] direction (Figure 2). The Fe–Fe interatomic distance in these chains is 2.5630(4) Å, only about 3% longer than the shortest Fe–Fe distance in α -Fe metal.¹⁴ Similar ${}^1_{\infty}[\text{Fe}_2\text{S}_4]$ chains are found in β - BaFe_2S_4 ² and in the other members of the adaptive series

$\text{Ba}_p(\text{Fe}_2\text{S}_4)_q$, for example, $\text{Ba}_5\text{Fe}_9\text{S}_{18}$ ($p = 5$ and $q = 9/2$).⁶ The shortest Fe–Fe distance in these compounds is 2.646(1) Å in β - BaFe_2S_4 .²

The Ba–I network that surrounds the ${}^1_{\infty}[\text{Fe}_2\text{S}_4]$ chains consists of one crystallographically independent Ba atom and two crystallographically independent I atoms. The Ba center sits on a site with m symmetry. Each Ba atom is surrounded by a distorted capped square antiprism composed of three S, one I(1), and five I(2) atoms. The I(1) atom sits on a site with $4/m$ symmetry at the center of a square plane of Ba atoms. This unusual coordination environment for I^- is not unprecedented. A square-planar configuration for I^- is also observed in the organometallic compound $[\text{K}(18\text{-crown}(6))][(\text{PhSbI}_2)_4\text{I}]$ ¹⁵ where I^- is coordinated by four PhSbI_2 units in a square-planar fashion.

There are no S–S bonds in the structure, so the formal oxidation state of the S is -2 . With formal oxidation states of Ba^{2+} and I^- there must be one Fe^{2+} and one Fe^{3+} ion per formula unit. As there is only one crystallographically independent Fe site, the average oxidation state of any given Fe atom is $+2.5$. The Fe–S bond distance of 2.267(2) Å is slightly longer than the Fe–S distance for Fe^{3+} in β - BaFe_2S_4 ² of 2.218(1) Å but may be shorter than the Fe–S distances for Fe^{2+} in Ba_2FeS_3 of 2.27(1) and 2.28(1) Å.³

Apart from the short Fe–Fe distance, all other distances are normal. The following comparisons can be made for Ba: Ba–S, 3.195(2)–3.298(1) Å vs 3.14(5)–3.48(5) Å in $\text{Ba}_5\text{Fe}_9\text{S}_{18}$;⁶ Ba–I, 3.5132(6)–3.7276(6) Å vs 3.513(3)–3.842(2) Å in $\text{Ba}_6\text{Pr}_3\text{I}_{19}$.¹⁶ All of these distances are close to those expected for van der Waals' interactions.

Mössbauer Spectra. The Mössbauer spectra (Figure 3) of $\text{Ba}_4\text{Fe}_2\text{I}_5\text{S}_4$ have been obtained at 4.2, 85, and 270 K and fit with one magnetic component at 4.2 K and one symmetric quadrupole doublet at the higher temperatures; the hyperfine parameters resulting from these fits are given in Table 3. Because of the presence of Ba^{2+} and I^- ions that produce extensive nonresonant scattering, the observed spectra have both a smaller percentage absorption and a lower signal-to-noise ratio than are usually observed for the spectra of iron sulfide compounds. As a consequence, several days were required to obtain each of the spectra shown in Figure 3.

The 85 and 270 K spectra are composed of a single symmetric quadrupole doublet, as would be expected for the single crystallographic Fe site found in $\text{Ba}_4\text{Fe}_2\text{I}_5\text{S}_4$. The isomer shift observed at 270 K corresponds to a valence of $+2.6(2)$ for the paramagnetic iron ion, as may be deduced from the room-temperature correlation reported earlier¹⁷ in closely related iron–sulfide compounds. This formal oxidation state is in good agreement with that of $+2.5$ dictated by charge balance in stoichiometric $\text{Ba}_4\text{Fe}_2\text{I}_5\text{S}_4$. As expected, the isomer shift increases upon cooling from 270 to 85 K as

(13) Gray, D. L.; Ibers, J. A. *J. Alloys Compd.* **2007**, *440*, 74–77.

(14) Jette, E. R.; Foote, F. *J. Chem. Phys.* **1935**, *3*, 605–616.

(15) Von, Seyerl, J.; Scheidsteger, O.; Berke, H.; Huttner, G. *J. Organomet. Chem.* **1986**, *311*, 85–89.

(16) Gerlitzki, N.; Mudring, A.-V.; Meyer, G. *Z. Anorg. Allg. Chem.* **2005**, *631*, 381–384.

(17) Hoggins, J. T.; Steinfink, H. *Inorg. Chem.* **1976**, *15*, 1682–1685.

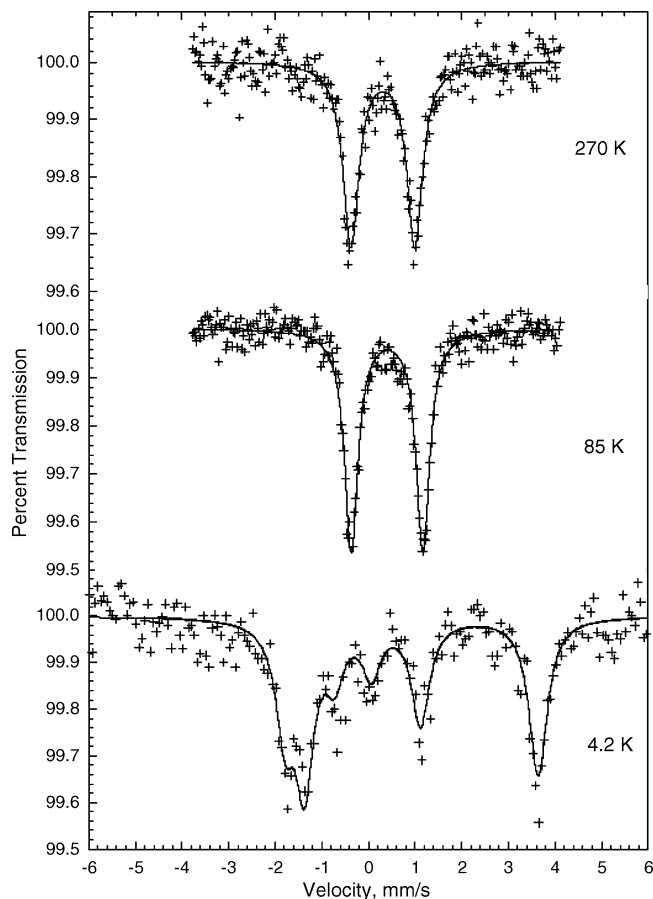


Figure 3. Mössbauer spectra of $\text{Ba}_4\text{Fe}_2\text{I}_5\text{S}_4$ obtained at the indicated temperatures.

Table 3. Mössbauer Spectral Parameters

T, K	hyperfine field H, T	isomer shift $\delta, \text{mm/s}^a$	quadrupole splitting $\Delta E_Q, \text{mm/s}$	line width $\Gamma, \text{mm/s}$
270	0	0.308	1.37	0.41
85	0	0.401	1.54	0.35
4.2	15.5	0.402	1.54 ^b	0.48
4.2	15.5	0.408	1.50 ^c	0.45

^a The isomer shifts are given relative to room-temperature α -Fe foil.

^b Parameter constrained to the value given. ^c Unconstrained fit.

a result of the second-order Doppler shift,¹⁸ and the observed increase is typical of compounds containing either Fe^{2+} or Fe^{3+} .

The sextet Mössbauer spectrum of $\text{Ba}_4\text{Fe}_2\text{I}_5\text{S}_4$ obtained at 4.2 K (Figure 3) clearly indicates the presence of long-range magnetic order, an order that magnetic susceptibility studies (see below) indicate is most likely antiferromagnetic ordering between the ${}^1_{\infty}[\text{Fe}_2\text{S}_4]$ chains at low temperature. Because of the small internal hyperfine field and the large quadrupole interaction, the magnetic spectrum must be fit by diagonalizing the ${}^{57}\text{Fe}$ nuclear ground and excited-state Hamiltonians and calculating the best-fit eigenvalues and eigenvectors. The resulting fits indicate that the asymmetry parameter η must,

as expected, be zero and that the angle θ between the principal axis of the electric field gradient and the easy axis of magnetization must be 0° ; alternative values of η and θ lead to very poor fits.

Surrounding the Fe center in $\text{Ba}_4\text{Fe}_2\text{I}_5\text{S}_4$ are the four tetrahedrally placed S atoms at 2.267(2) Å and two next-nearest-neighbor Fe atoms at $\pm 2.5630(4)$ Å ($\pm c/2$) along the ${}^1_{\infty}[\text{Fe}_2\text{S}_4]$ chains; the next-closest near neighbors are four Ba atoms at 3.7897(6) Å. Thus, these two Fe atoms at $\pm c/2$ in the ${}^1_{\infty}[\text{Fe}_2\text{S}_4]$ chains yield, at least in part, the principal component of the electric field gradient, a gradient that is axial and, as expected, oriented along the crystallographic c axis. Then the magnetic easy axis in $\text{Ba}_4\text{Fe}_2\text{I}_5\text{S}_4$ must be parallel to the ${}^1_{\infty}[\text{Fe}_2\text{S}_4]$ chains because θ is 0° .

The observation of a single quadrupole doublet at 85 and 270 K, as well as a single magnetic component at 4.2 K (see below), indicates that at these temperatures the electron delocalization between the nominally Fe^{2+} and Fe^{3+} ions is rapid as compared to the 10^{-7} s lifetime of the ${}^{57}\text{Fe}$ $I = 3/2$ nuclear excited state. The observed quadrupole splitting of 1.54 mm/s at 85 K is somewhat larger than would be expected for the essentially tetrahedral FeS_4 coordination found in the structure at 153 K.

Isomer Shifts. If, as seems likely, there is rapid electron delocalization on the Mössbauer time scale, then the observed hyperfine parameters for $\text{Ba}_4\text{Fe}_2\text{I}_5\text{S}_4$ should be approximately the 50:50 time-averaged values of the hyperfine parameters of Fe^{2+} in Ba_2FeS_3 and Fe^{3+} predicted¹⁷ for Ba_3FeS_5 because these compounds also contain nearly tetrahedral FeS_4 units. The average of the isomer shifts observed^{4,9} in Ba_2FeS_3 and Ba_3FeS_5 is 0.39 mm/s at 300 K and 0.50 mm/s at 78 K compared with those of 0.308 and 0.401 mm/s (Table 3) found in $\text{Ba}_4\text{Fe}_2\text{I}_5\text{S}_4$ at 270 and 85 K, respectively. Furthermore, if one assumes that all the quadrupole splittings have the same sign, then the average of the quadrupole splittings observed^{4,9} in Ba_2FeS_3 and Ba_3FeS_5 is 1.53 mm/s at 300 K and 1.67 mm/s at 78 K; these values may be compared to those of 1.37 and 1.54 mm/s found here (Table 3) at 270 and 85 K, respectively. We thus conclude that the parameters observed for $\text{Ba}_4\text{Fe}_2\text{I}_5\text{S}_4$ are consistent with the rapid electron delocalization expected in this compound.

Taft and co-workers^{19–22} have carried out spin-polarized multiple-scattering and Slater X α local exchange calculations of the electronic structures of the tetrahedral $[\text{FeS}_4]^{4-}$, $[\text{FeS}_4]^{5-}$, and $[\text{FeS}_4]^{6-}$ anions (Table 4). They find that in going from $[\text{Fe}^{2+}\text{S}_4]^{6-}$ to $[\text{Fe}^{3+}\text{S}_4]^{5-}$ there is relatively little change in the Fe electronic configuration and that the Fe net charge, rather than going from +2 to +3, increases only slightly from +1.07 to +1.20. Likewise, in going from $[\text{Fe}^{3+}\text{S}_4]^{5-}$ to $[\text{Fe}^{4+}\text{S}_4]^{4-}$, there is again little change in the Fe configuration, presumably as a result of extensive “back-

(19) Taft, C. A.; Braga, M. *Phys. Rev. B* **1980**, *21*, 5802–5807.

(20) Lie, S. K.; Taft, C. A. *Phys. Rev. B* **1983**, *28*, 7308–7316.

(21) Taft, C. A.; Raj, D.; Danon, J. J. *Phys. Colloq.* **1974**, *6*, 241–245.

(22) Cooper, D. M.; Dickson, D. P. E.; Domingues, P. H.; Gupta, G. P.; Johnson, C. E.; Thomas, M. F.; Taft, C. A.; Walker, P. J. *J. Magn. Mater.* **1983**, *36*, 171–174.

(18) Shenoy, G. K.; Wagner, F. E.; Kalvius, G. M. In *Mössbauer Isomer Shifts*; Shenoy, G. K., Wagner, F. E., Eds.; North-Holland Publishing Company: Amsterdam, The Netherlands, 1978; p 51.

Table 4. Calculated Electronic Properties of Some Iron–Sulfur Anions^a

anion	Fe electronic configuration	Fe charge	$\rho(0)$, e/a ₀ ³	$\rho(0)$, e/a ₀ ³ relative to α -Fe	δ , mm/s
[Fe ²⁺ S ₄] ⁶⁻	3s ^{1.98} 3p ^{5.92} 4s ^{0.81} 3d ^{6.22}	+1.07	11 875.98	-2.02	0.404
[Fe ³⁺ S ₄] ⁵⁻	3s ^{1.98} 3p ^{5.92} 4s ^{0.85} 3d ^{6.05}	+1.20	11 876.37	-1.63	0.326
[Fe ⁴⁺ S ₄] ⁴⁻	3s ^{1.98} 3p ^{5.93} 4s ^{0.89} 3d ^{5.98}	+1.22	11 877.80	-0.20	0.04

^a References 19–22**Table 5.** Calculated α - and β -Spin Electronic Configurations and Hyperfine Fields of Some Iron–Sulfur Anions^a

anion	Fe α -spin electronic configuration	Fe β -spin electronic configuration	H_c , T
[Fe ²⁺ S ₄] ⁶⁻	3s ^{0.99} 3p ^{2.96} 4s ^{0.40} 3d ^{4.83}	3s ^{0.99} 3p ^{2.96} 4s ^{0.41} 3d ^{1.39}	-27.3
[Fe ³⁺ S ₄] ⁵⁻	3s ^{0.99} 3p ^{2.97} 4s ^{0.43} 3d ^{4.94}	3s ^{0.99} 3p ^{2.95} 4s ^{0.42} 3d ^{1.11}	-25.0
[Fe ⁴⁺ S ₄] ⁴⁻	3s ^{0.99} 3p ^{2.97} 4s ^{0.44} 3d ^{4.63}	3s ^{0.99} 3p ^{2.96} 4s ^{0.45} 3d ^{1.35}	-21.6

^a References 19–22.

donation” of electron density from a S 3p orbital onto the Fe ion. As a consequence, the charge on the Fe again increases only slightly from +1.20 to +1.22. Thus, the observed isomer shift in a formally Fe⁴⁺ compound, such as Ba₃FeS₅, is usually very similar to that of a formally Fe³⁺ compound. Indeed, because of these small changes the range of ⁵⁷Fe isomer shifts is smaller than would be expected in formally Fe²⁺, Fe³⁺, and Fe⁴⁺ compounds. Furthermore, because of the extensive covalence in these tetrahedral anions, the actual isomer shifts are smaller than expected for non-sulfide Fe²⁺, Fe³⁺, and Fe⁴⁺ compounds.

Of course, the isomer shift depends upon the *ns* electron density, $\rho(0)$, at the ⁵⁷Fe nucleus as compared to that of α -Fe, where the proportionality constant²¹ between the isomer shift and $\rho(0)$ is ca. -0.2 (mm/s)/a₀³. The calculated $\rho(0)$ values (presumably at 0 K) for the three anions are given in Table 4. By using the value for $\rho(0)$ of 11 878 e/a₀³ for α -Fe,²³ one obtains the calculated values of $\rho(0)$ and the corresponding isomer shifts relative to α -Fe for the [FeS₄]⁴⁻, [FeS₄]⁵⁻, and [FeS₄]⁶⁻ anions (Table 4). Thus, relative to these calculated isomer shifts, that of 0.402 mm/s observed at 4.2 K for Ba₄Fe₂I₅S₄ is in the expected range of those for [Fe²⁺S₄]⁶⁻ and [Fe³⁺S₄]⁵⁻, albeit much closer to that for [Fe²⁺S₄]⁶⁻.

Hyperfine Field. The hyperfine field of 15.5 T observed in Ba₄Fe₂I₅S₄ at 4.2 K is much smaller than the typical Fe³⁺ hyperfine field but is similar to the 15.6 and 17.7 T fields observed⁹ in Ba₆Fe₈S₁₅ at 78 K, a compound with an average Fe oxidation state of 2.25 as dictated by charge balance and an oxidation state of 2.43 as determined from the correlation of isomer shifts.¹⁷ In contrast, the 15.5 T field observed in Ba₄Fe₂I₅S₄ at 4.2 K is substantially smaller than the 24–29 T fields observed in Ba₇Fe₆S₁₄ at 78 K, a compound with an average Fe oxidation state of 2.33 from charge balance and 2.49 from the isomer shift correlation.¹⁷ Because the hyperfine field at isolated Fe ions is known to be negative, in the following discussion it has been assumed that the observed field in Ba₄Fe₂I₅S₄ at 4.2 K is -15.5 T.

Taft and co-workers^{19–22} have also determined (Table 5) the α - and β -spin, or more commonly the spin-up and spin-

down, electronic configurations of the tetrahedral [FeS₄]⁴⁻, [FeS₄]⁵⁻, and [FeS₄]⁶⁻ anions. Once again, except for the 3d populations, the results for the three anions are surprisingly similar.

The observed effective hyperfine field, H_{eff} , exhibited by Fe is given by $H_{\text{eff}} = H_c + H_{\text{orb}} + H_{\text{dip}}$, where H_c is the Fermi contact contribution to the field, a contribution that is proportional to the difference in the α - and β -electron spin densities at the ⁵⁷Fe nucleus, and H_{orb} and H_{dip} are the orbital and dipolar contributions to the effective field. The latter contributions are expected to be small, ca. 2 T for Ba₄-Fe_{2.5+}I₅S₄, and of opposite sign to that of H_c .

The calculated core hyperfine fields of the [FeS₄]⁴⁻, [FeS₄]⁵⁻, and [FeS₄]⁶⁻ anions (Table 5) as well as the hyperfine field observed at 4.2 K for Ba₄Fe₂I₅S₄ are much less negative than the calculated H_c values of -57.7, -78.3, and -64.8 T for isolated Fe²⁺, Fe³⁺, and Fe⁴⁺ ions. This suggests strong covalency in the Fe–S bonds. The calculated fields indicate that, as expected, small variations in the Fe 3d populations and spin-polarizations in the [FeS₄]^{*n-*} anions can induce substantial changes of several tesla in the Fe 3s and 4s polarization contributions to H_c .

The field of -15.5 T observed in Ba₄Fe₂I₅S₄ at 4.2 K is less negative than all the calculated core fields and is similar to the -15 T²¹ or -19.5 T²² fields observed in CsFeS₂. In order to reduce the absolute value of the field in Ba₄Fe₂I₅S₄, either H_{dip} and H_{orb} must be more positive than usual or the electronic configuration of Ba₄Fe₂I₅S₄ must differ from the calculated anion configurations, as shown above in the isomer shift comparison.

The less negative calculated core fields, as compared to the Fe free ion core fields, result from an increase in both the 3d and 4s populations in the [FeS₄]^{*n-*} anions. An even larger 3d and 4s population in Ba₄Fe₂I₅S₄ would lead to a less negative effective hyperfine field. If we assume that the difference between the calculated fields given in Table 5 and the observed field of -15.5 T in Ba₄Fe₂I₅S₄ results from an additional 4s spin density, a ξ value¹⁹ of 2.9 is obtained, where $\xi/4\pi$ is the difference in the *ns* α -spin and β -spin densities at the ⁵⁷Fe nucleus. This ξ value corresponds to a transfer of 0.12 electrons between these orbitals. An increase in the 3d β -spin population would reduce the magnitude of the negative and positive 2s and 3s spin contributions. Such an increase in the 3d population would also increase the isomer shift from the intermediate value of 0.365 mm/s (Table 4) to the observed value of 0.402 mm/s at 4.2 K.

Magnetic Properties. The magnetic properties of Ba₄-Fe₂I₅S₄ powder, obtained between 3.4 and 300 K, are shown in Figure 4. The molar magnetic susceptibilities, χ_M' , obtained

(23) Watson, R. E. *Phys. Rev.* **1960**, *118*, 1036–1045.

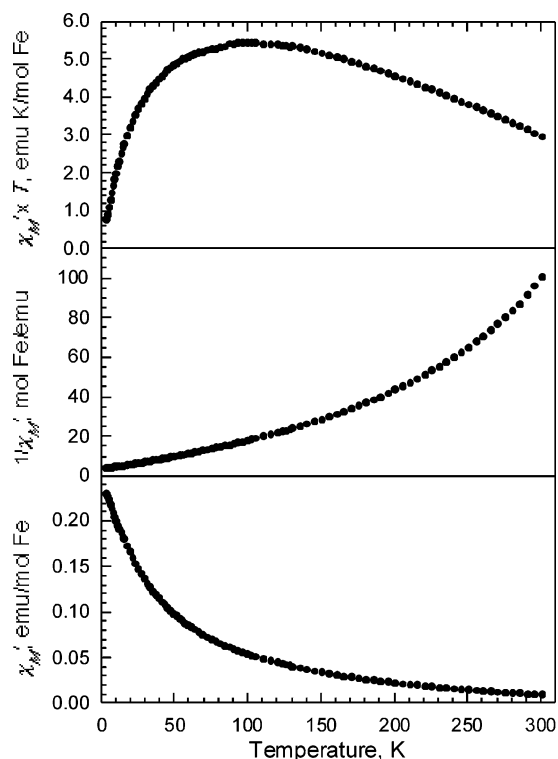


Figure 4. Magnetic properties per Fe of $\text{Ba}_4\text{Fe}_2\text{I}_5\text{S}_4$ obtained between 3.4 and 300 K.

after zero-field cooling and after field cooling in a 0.7 T applied field were the same within experimental error and have been merged.

The curvature observed in $1/\chi_M'$ vs T (Figure 4) of $\text{Ba}_4\text{Fe}_2\text{I}_5\text{S}_4$ indicates that Curie-law behavior between 3.4 and 300 K is not obeyed. Rather, the magnetic properties of $\text{Ba}_4\text{Fe}_2\text{I}_5\text{S}_4$ may result from a combination of one- and three-dimensional magnetic exchange and, perhaps less likely, zero-field splitting. Because of the difficulty in modeling the one-dimensional ferromagnetic exchange interactions, which presumably arise predominately from the delocalization of unpaired electrons along the Fe^{2+} $S = 2$ and Fe^{3+} $S = 5/2$ linear chains (Figure 2), we have been unable to obtain a quantitative evaluation of the magnetic exchange coupling and the zero-field splitting present. Insofar as we know, there is no theoretical treatment of this type of one-dimensional magnetic exchange interaction.

Qualitatively we believe, on the basis of the increase in $\chi_M' T$ between 300 and 100 K (Figure 4), that there may be weak pseudo-one-dimensional ferromagnetic exchange coupling along the linear chains as a result of double exchange in the presence of electron delocalization.²⁴ Then at lower temperatures, on the basis of the decrease in $\chi_M' T$ between 100 and 3.4 K, there may be weak antiferromagnetic exchange coupling between the chains, chains that are separated by an $\text{Fe}\cdots\text{Fe}$ distance of 9.729 Å. Furthermore, there is no indication of a maximum in χ_M' , i.e., a Curie or Néel temperature, between 3.4 and 300 K, as would be expected for a pseudo-one-dimensional interaction. Because

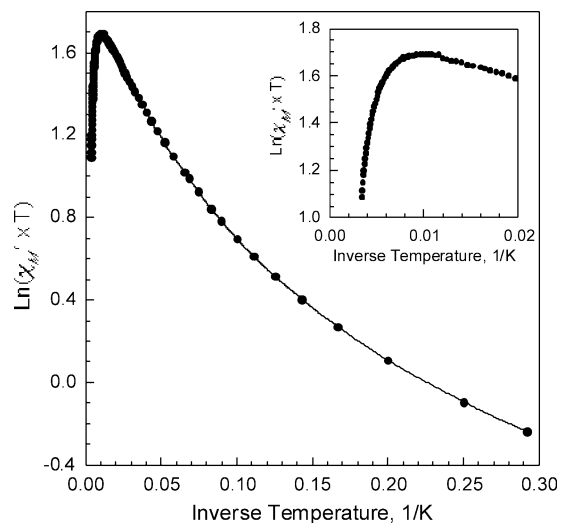


Figure 5. Inverse temperature dependence of $\ln(\chi_M' T)$ obtained between 300 and 3.4 K and between 300 and 50 K (inset).

the interchain antiferromagnetic exchange coupling is probably much weaker than the intrachain ferromagnetic exchange coupling, it is possible that the expected Néel point is not observed. Alternatively, the antiferromagnetic ordering temperature may occur below 3.4 K. Indeed, in one-dimensional antiferromagnetic systems, a maximum in χ_M' typically occurs²⁵ at kT_{max} between J and $10J$, where J is the interchain antiferromagnetic exchange coupling constant. Thus, it follows that J could be smaller than ca. 0.34–3.4 K. For orbitally nondegenerate Fe^{3+} interactions, the decrease in $\chi_M' T$ with decreasing temperature is consistent with the presence of populated lower spin-multiplicity states at the lower energies as a result of antiferromagnetic interactions. For orbitally degenerate Fe^{2+} interactions, the decrease in $\chi_M' T$ with decreasing temperature is also consistent with the possible presence of a small negative zero-field splitting, D .

Finally, we note that the plot of $\ln(\chi_M' T)$ vs $1/T$ (Figure 5) shows features that are apparently unique for pseudo-one-dimensional magnetic interactions,²⁶ namely, the nonlinearity at higher temperatures and the rapid decrease at low temperatures.

The presence of antiferromagnetic exchange at lower temperatures is consistent with the long-range magnetic order observed in the Mössbauer spectrum obtained at 4.2 K (Figure 3). Of course, some undetermined portion of the decrease in $\chi_M' T$ at the lower temperatures may also arise from the presence of a small zero-field splitting, D , resulting from the slight distortion of the FeS_4 tetrahedron from perfect T_d symmetry.

Surprisingly, there is no indication of long-range magnetic ordering in the Mössbauer spectra of $\text{Ba}_4\text{Fe}_2\text{I}_5\text{S}_4$ obtained at 85 or 270 K. This must indicate that the one-dimensional magnetic exchange correlation distances along the linear chains are small and that the moments are rapidly relaxing

(24) Zener, C. *Phys. Rev.* **1951**, *82*, 403–405.

(25) Hatfield, W. E. In *Solid State Chemistry: Techniques*; Cheetham, A. K., Day, P., Eds.; Oxford University Press: New York, 1987.

(26) Coulon, C.; Miyasaka, H.; Clérac, R. *Struct. Bonding (Berlin)* **2006**, *122*, 163–206.

relative to the ^{57}Fe Larmor precession frequency of ca. 0.5×10^{-8} s at and above 85 K. The Fe electron delocalization along the linear chain may help induce the short correlation length and thus the relatively fast relaxation.

Acknowledgment. The authors thank Dr. B. Bartlett for useful discussions during the course of this work. Funding for this work was kindly provided by U.S. Department of Energy Grant No. BES ER-15522 and the Fonds National de la Recherche Scientifique, Belgium, through Grant Nos. 9.456595 and 1.5.064.05. Use was made of the Jerome B. Cohen X-ray facility supported by the U.S. National Science

Foundation at the MRSEC of Northwestern University under Grant No. DMR05-20513.

Note Added after ASAP Publication. This paper was released ASAP on December 6, 2007, without a current address for one of the authors. The corrected version was posted on December 7, 2007.

Supporting Information Available: The crystallographic file in CIF format for $\text{Ba}_4\text{Fe}_2\text{I}_5\text{S}_4$. This material is available free of charge via the Internet at <http://pubs.acs.org>.

IC701085C